Chapter 3
Model validation: comparison with observed carbon dynamics data on the plot scale

3.1. Introduction

All models must be validated by examining the capability to capture the actual features, at least in a qualitative manner. However, especially for global carbon cycle models, validation is one of the most difficult points, because of the data deficiency. Ideally, a model should use two independent datasets: one is for model calibration and another for model validation. With respect to the carbon cycle model, filed measurements of carbon fluxes and pools are definitely far from abundance, such that they cover only a tiny fraction of land area. In the International Biological Programme (IBP) which was launched in 1965 and continued to 1974, a large amount of data were gathered from a variety of biomes, in order to appraise the potential dry-matter productivity of the biosphere. In consequence, hundreds of *NPP* data were collected by a large number of ecologists and agronomists, and were synthesized into an empirical model of *NPP* estimation (Lieth, 1975). Nevertheless, the IBP data have only a limited applicability to the global change study to date, because; (1) in the IBP field studies, the soundest ecosystems were deliberately chosen, although they were not representative to respective biomes; (2) only *NPP* was comprehensively addressed, rather than holistic ecosystem processes; (3) in most cases, these studies focused on the average aspects and then paid little attention to their year-to-year and decadal variability; (4) physiological mechanisms underlying the productivity were not fully explored; and (5) these data were heterogeneous in their accuracy and geographical distribution, due to practical methodological problems. Indeed, there are only a few studies, which explored carbon dynamics of terrestrial ecosystems entirely from photosynthetic assimilation to respiratory emission. Because these data should be used to construct and calibrate the model, we can not make a comparison with independent data. However, we regard that a high correlation between model estimates and

the field observations is essential and sometimes sufficient, to validate the model.

3.2. Simulation design

Two lines of simulation would show the validity of Sim-CYCLE, with respect to the capability to capture the actual carbon dynamics. (I) At four representative sites, in which carbon fluxes and pools were comprehensively measured, we conduct a comparison between model estimation and filed data. (II) At worldwide 21 sites (including the four sites mentioned above), in which at least a part of carbon dynamics was measured, we conduct a comparison for such typical aspects as *NPP*, *LAI*, plant biomass and soil carbon storage. The global distribution of these sites is shown in Fig. 3-1.

In each of the experimental sites, Sim-CYCLE should retrieve the ecosystem features in 1960s to 1970s, when most of the field data were collected. Correspondingly, atmospheric CO_2 concentration is fixed as 335 ppmv, the level around 1980 (Keeling et al., 1989), and climate condition is the long-term average of the period from 1961 to 1998. All of the climate and soil conditions in this section are derived from global datasets (see Chapter 4), so that the plot-scale validation is more relevant to the global-scale simulation. Calculation is launched from the juvenile stage, where initial carbon content is 0.1 Mg C ha^{-1} for each compartment, and repeated for a sufficiently long period to attain the equilibrium state under a stationary environmental condition. Annual *NEP* is used as the criteria to determine whether the ecosystem carbon dynamics is sufficiently equilibrated (i.e. climax stage): $NEP<0.0001$ Mg C ha^{-1} yr^{-1}.

3.2.1. Description of the four representative sites

The representative characteristics in each of the four example sites are listed in Table 3-1 and explained below. Figure 3-2 shows the seasonal change in environmental conditions (temperature, water, and light) in each site.

(1) Tropical rain forest site (TRF) This site locates in southern Peninsular Malaysia (2° 58'N 102° 18'E, 100 m above sea level), in Pasoh National Forest. The site is under humid

tropical climate; annual mean air temperature *TA* is 24.8 °C (from 24.0 °C in Dec. to 25.4 °C in May) and annual precipitation *PR* is 1719 mm (at least 100 mm for each month). Thus, this site lacks apparent seasonality in climate (e.g. no apparent dry season) and plant phenology. There occur silty loam Tropudults, with a relatively shallow rooting zone. One of a few studies of direct (i.e. destructive) measurement of biomass and *NPP* in a pristine tropical forest was performed by the Japanese IBP group in 1973 (Kira, 1987). They revealed that the plot is one of the most productive ecosystems in the world. The site was covered with pristine lowland tropical rain forest and composed of diverse evergreen broad-leaved species (e.g., 277 woody species in 2-ha plot), including Dipterocarpaceous species typical for tropical rain forests. The canopy of the forest reaches as high as 50 m above the floor, and develops a vertical stratified structure.

(2) Warm-temperate evergreen broad-leaved, or lucidophyll forest site (LPF) This site locates in Minamata, Japan (32°10'N 130°28'E), at the west slope of a ridge of Kunimi Mountains (400-637 m above sea level). This site is under typical Asian Monsoon climate; annual mean *TA* is 17.9 °C (from 10.0 °C in Jan. to 26.6 °C in Aug.) and annual *PR* is 1207 mm (with an apparent rainy season in Jun. to Aug.). There occurs semi-dry or mesic subtype of brown forest soil mostly generated from andesite; the warm and perhumid climate may make a well-developed rooting zone. Kira et al. (1978) presented the synthesis of the project studies by JIBP from 1967 to 1973, including floristic description, productivity, and matter cycle. The forest is a secondary forest, and covered with lucidophyll (i.e. temperate evergreen broad-leaved) tree species. Especially at higher altitudes, it is predominated by such evergreen species as *Castanopsis cuspidata*, *Quercus glauca*, *Q. myrsinaefolia*, and *Machilus thunbergii*, with some mixture of deciduous broad-leaved species.

(3) Boreal deciduous needle-leaved forest site (BLF) This site locates in Aldan Plateau, eastern Siberia (60°51'N 128°16'E, 300 m above sea level). A northern continental climate predominates there; annual mean *TA* is –9.3 °C (from –35 °C in Jan. to 18.0 °C in

Aug.) and annual *PR* is as low as 274 mm. There occurs peaty Inceptisol, with a silt loam texture. Schulze et al. (1995) reported that the site was a typical boreal deciduous forest occupied by larch, *Larix gmelinii*, with such understorey species as *Vaccium vitis-idaea* and *Ledum palustre*. The presence of permafrost is essential for the formation of forest ecosystem, which generally occurs in moist to wet habitat, by mediating water condition. Growing-period (*TA*>5°C) is restricted from June to August, while day-length is as long as 15 to 20 hours. Schulze et al. (1995) present information on biomass, *LAI*, and soil carbon content at the study site, and Schulze et al. (1999) on productivity of Siberian larch forests. They suggest that biomass and *LAI* in larch forest may be markedly different between young and mature stands.

(4) Tall grassland site (WTG) This site locates in Osage, Oklahoma, U.S.A. (36°57'N 96°33'W, 380 m above sea level). A moderately arid climate predominates there; annual mean *TA* is 14.3 °C (from -0.4 °C in Jan. to 28.1 °C in Jul.) and annual *PR* is 575 mm (relatively rainy in summer). However, annual precipitation is highly changeable year by year, ranging from 400 to 800 mm (Sims and Coupland, 1979). There occurs an arid-type silty clay soil, Brunizem, with a moderate rooting depth and *WHC*. Sims and Coupland (1979) presented the synthesis of grassland studies by IBP groups, including one by the U.S. group in Great Plains. The site is classified into true prairie and composed of tall grasses, including both C_3 and C_4 species; the predominant species are *Andropogon gerardi* and *Panicum virgatum*. According to French (1979), up to 58 % of plant species in the Osage site was composed of C_4 species.

3.2.2. Description of 21 validation sites

From a large amount of literature, 21 sites (including four sites, mentioned above) were selected, in which at least a part of carbon dynamics was measured in the ecological way. Then, these sites include several IBP sites. The data reference for each site is as follows (those for the four exemplified sites have already given above): tussock tundra in Eagle creek, USA,

from Shaver and Chapin (1980, 1986) and Miller et al. (1984): tundra in Toolik Lake, USA, from Giblin et al. (1991) and Shaver and Chapin (1991): boreal evergreen forest in Ruissia from Schulze et al. (1999) and Wirth et al. (1999): temperate needle-leaved forest (scot pine) in Solling, Germeny, from Bredemeier et al. (1995), Tiktak and van Grinsven (1995) and Tiktak et al. (1995): grasslands in the Great Plains, i.e. Matador, Pawnee, and San Joaquin, USA, from Sims and Coupland (1979) and Parton et al. (1993): temperate needle-leaved forest (*Tsuga* spp.) in the Oregon Transect, USA, from Runyon et al. (1994): temperate deciduous broad-leaved forest in Hubbard Brook, USA, from Whittaker et al. (1974): temperate deciduous broad-leaved forest in Oak Ridge, USA, from Whittaker (1975): temperate needle-leaved forest (Douglas fir) on Mt. Taylor, USA, from Gower et al. (1992): warm-temperate broad-leaved evergreen forest on Mt. Kasuga, Japan, from Yoda (1971): warm-temperate oak forest in Kilbury (at the base of the Himalaya), India, from Rawat and Singh (1988): tropical dry forest in Marihan, India, from Singh and Singh (1991): tropical rain forest in Khao Chong, Thailand, from Ogawa et al. (1965a, b) and Kira et al. (1967): tropical rain forest in Manaus, Brazil, from McWilliams et al. (1993): and tropical savanna in Nylsvley, South Africa, from Raich et al. (1991). In temperate grassland sites, Matador, Pawnee, and San Joaquin, C_3/C_4 plants composition was derived from French (1979) (0, 52, and 50 %, respectively), similar to the WTG site.

For each of the 21 sites, their location, dominant biome type, and climate condition are briefly described in Table 3-2. It is expected that these sites should cover a wide variety of biomes as much as possible, although actually they lack sites at desert, wetland, mixed forest, and cropland. The comparison was made in the 21 sites for annual *NPP*, the 11 sites for *LAI*, the 18 sites in plant C, and the 14 sites for soil C (some sites lack data items). The 21 sites cover a wide range of biomes, from arctic tundra to tropical rain forest. Annual temperature differs among the sites, from –9.3 °C in Russian larch forest to 26.7 °C in Thai tropical rain forest, and annual precipitation ranges from 275 mm in Russian larch forest to 3290 mm in Brazilian tropical rain forest. Although all ecosystems do not always reach their climax stage due to some disturbance effect, all the data were regarded as equilibrium carbon dynamics, to

simplify interpretation of the simulation.

3.3. Results

3.3.1. At the four representative sites

3.3.1.1. Validity of environmental submodules

The radiation and hydrological submodules realized well habitat conditions in each of the four example sites. Seasonal change in *DL* and $PPFD_{MD}$ seemed valid, such that *DL* changed little in the TRF site (from 11.8 to 12.2 hours) and changed largely in the BLF site (from 4.7 to 19.3 hours). In the WTG site, average $PPFD_{MD}$ was highest (1427 μmol photons m^{-2} s^{-1}) among the four sites, due to the lower cloudiness. Figure 3-3 shows that the water budget differed markedly among the four example sites. In the TRF and LPF sites, a substantial amount of water was lost through interception *IC*, transpiration *TR*, and runoff *RO*, whereas little evaporation *EV* occurred. In the BLF and WTG sites, where precipitation was relatively low, water loss by *EV* had the largest contribution, and loss by *RO* was negligible. The ratio of *AET* to *PET* clarifies the difference in water availability: humid in the TRF and LPF sites (*AET/PET* ≅ 1.0) and arid in the BLF and WTG sites (*AET/PET* ≅ 0.6).

3.3.1.2. Carbon budget at the equilibrium

Ecophysiologocal parameters in Sim-CYCLE were carefully tuned site-by-site, so that equilibrium carbon dynamics was successfully simulated (Table 3-3). At first, the site-specific difference was apparent in the time to reach the equilibrium state, from 366 years in the TRF site to 2450 years in the BLF site (Table 3-4). This difference was not related to the magnitude of the carbon storage capacity itself; indeed, the BLF site had the lowest carbon density (161.5 Mg C ha^{-1} yr^{-1}). Figures 3-4 and 3-5 show that transition of carbon fluxes and carbon storage was appropriately retrieved by Sim-CYCLE in each of the four example sites (exemplified for the first 100 years). *NPP* had the highest value in the young stage, due to both lower *ARM* and higher *GPP*, and then decreased to the static value (Fig. 3-4). (Irregular *NPP* variation in the BLF and WTG sites during the first 5 years may be, at least in part, an

artifact of the simulation). Similarly, *NEP* had very high values at first (e.g. 10 Mg C ha^{-1} yr^{-1}), and gradually decreased to zero (i.e. the magnitude of annual *NPP* and *HR* became close each other). The equilibrium carbon dynamics was obviously different among the four sites (Table 3-4). Annual *NPP* ranged from 2.2 Mg C ha^{-1} yr^{-1} in BLF site to 10.8 Mg C ha^{-1} yr^{-1} in the TRF site, and *WE* ranged from 161.5 Mg C ha^{-1} in the BLF site to 321.3 Mg C ha^{-1} in the TRF site (Fig. 3-6). In spite of the lowest productivity and carbon storage, the BLF site had the highest dry-matter production efficiency (*NPP/GPP*) among the four sites, owing to the small respiratory carbon loss. The grassland WTG site had the lowest plant biomass but the largest soil carbon storage, because lower soil water availability restricted decomposition. The majority of *NPP* in the WTG site was performed by C_4 species (2.6 out of 4.0 Mg C ha^{-1} yr^{-1}), although they had a shorter growing period (9 months) than C_3 species (10 months). Accordingly, the WTG site shows the highest water use efficiency, compared with other forest sites. From the point of radiation use, the four experimental sites are divided into two groups (Table 3-4): the TRF and LPF sites, which have a dense and evergreen canopy (*LAI*=5-7) and higher *RUE*s: and the BLF and WTG sites, which have a sparse and deciduous canopy (*LAI*=1-2) and lower *RUE*s. In comparison with field measurements, we conclude that simulated carbon dynamics was sufficiently close to the actual one (Fig. 3-7). Although the model considerably underestimated *GPP* and *AR* in the TRF site, Sim-CYCLE gave convincing estimations of *LAI*, carbon storage, and carbon fluxes. For example, the total carbon storage of 307.2 Mg C ha^{-1} in the LPF site agreed with the observed value in a few percent. As shown in Fig. 3-8, seasonal variation in carbon fluxes was adequately captured. In the BLF and WTG sites, which are composed of deciduous species, *LF* showed a keen peak in their termination of growing-period. In the LPF and WTG sites, which are in temperate regions, net CO_2 uptake occurred mainly in their early growing-period; this may be in accordance with the seasonal change in atmospheric CO_2 concentration. Such agreement in various aspects of ecosystem carbon dynamics will support the model validity in a stronger manner than the comparison of *NPP* only.

3.3.2. At the worldwide 21 sites

As a consequence of parameter calibration (values not shown), Sim-CYCLE retrieved adequately carbon dynamics in the worldwide 21 sites. Figure 3-9 shows the correlations between field measurement and Sim-CYCLE estimation, for annual *NPP*, *LAI*, plant biomass, and soil carbon storage, respectively. *NPP* by Sim-CYCLE had a correlation coefficient (r^2) of as high as 0.996; then, most estimations were within ±10 % of the measured value. Plant biomass and soil carbon storage were also satisfactorily captured (r^2=0.999). For *LAI*, correlation was slightly low (r^2=0.958), partly because of the smaller number of data (n=11), but Sim-CYCLE could express the six-fold difference of *LAI* among the sites, ranging from 1.7 to 10.8.

3.4. Discussion

In both of the two lines of validation, estimated carbon dynamics agreed satisfactorily with measurements, suggesting that Sim-CYCLE is a viable tool to simulate terrestrial ecosystems. It can be seen from Fig. 3-9 that there is no bias in the estimated carbon dynamics from a wide variety of biomes. The biome-to-biome difference and seasonal change in carbon dynamics (i.e. Figs. 3-6 and 3-8) were properly retrieved by Sim-CYCLE; these points will be addressed at the global scale in the following chapters. For example, there is an apparent difference in the time to reach equilibrium among the experimental sites, probably attributable to the differences in the amount and activity of soil organic matter (cf. Figs. 3-4 and 3-5).

Nevertheless, it should be noted again that this agreement resulted from the calibration process (i.e. parameters were deliberately adjusted to capture the observations), without using an independent dataset. A number of data were not from a recent study but from the classic study (i.e. IBP), and then there may be difference in methodology and accuracy of measurement. Fortunately, the data deficiency is being ameliorated by the ongoing research projects, e.g. the International Geosphere-Biosphere Programme (IGBP) and the worldwide network of flux measurement (FLUXNET). The Data and Information System (DIS), a

project of the IGBP, is expected to construct a database of *NPP* covering a wide variety of biomes (this research is coordinated by the U.S. Oak Ridge National Laboratory). The FLUXNET is attempting to obtain fundamental information on the atmosphere-biosphere exchange of energy, water, and CO_2 (Baldocchi et al. 1996), and to scale up the information to the regional and continental scales, by coupling with remote sensing data (Running et al. 1999). These efforts will provide worthy information to examine the *NPP* and *NEP* estimated by ecosystem models like Sim-CYCLE, in a sophisticated manner. In contrast, there remains greater difficulty in validating carbon dynamics and leaf area index, because we do not have convenient and precise methods to measure them, especially underground carbon storage (root and soil organic matter). Sometimes, a surrogate method, i.e. comparison with other model estimations, may be sufficient to confirm whether a model behaves in a moderate or an extreme manner.

Table 3-1. Site conditions in four example sites

Item	Units	Site			
		Pasoh	Minamata	Yakutsk	Osage
		TRF	LPF	BLF	WTG
latitude	degree	2° 58' N	32° 10' N	60° 51' N	36° 57' N
longitude	degree	102° 18' E	130° 28' E	128° 16' E	96° 33' W
altitude	m	100	400	300	380
annual mean air temperature	℃	24.8	17.9	-9.3	14.3
annual precipitation	mm	1723	1211	275	579
annual mean cloudiness	fraction	0.70	0.60	0.43	0.33
soil hydraulic conductivity	10^{-3} day^{-1}	3.660	4.060	3.044	5.165
soil water holding capacity	mm	1001	1846	376	968

Table 3-2. Description of 21 plot-scale validation sites.

	Site	Biome	Lat.		Lon.		Annual climate Tem. (℃)	Annual climate Pre. (mm)	Observed carbon dynamics NPP (Mg C ha^{-1} yr^{-1})	LAI	WP (Mg C ha^{-1})	WS (Mg C ha^{-1})
	Eagle Creek, USA	tundra	65	10 N	145	30 W	-6.5	487	1.0	-	-	235.0
	Toolik Lake, USA	tundra	62	26 N	145	30 W	-6.5	487	0.7	-	3.9	74.4
*	Yakutsk, Russia (BLF)	boreal larch forest	60	51 N	128	16 E	-9.3	275	1.2	1.7	-	-
	Yenisei, Russia	boreal evergreen forest	60	43 N	89	8 E	-4.5	612	4.3	2.5	91.9	65.5
	Solling, Germany	temperate needle-leaved forest	51	40 N	9	30 W	8.4	737	5.2	5.9	143.8	95.0
	Matador, Canada	mixed prairie	50	42 N	107	48 W	4.1	458	3.2	-	10.9	-
	Oregon Transect, USA	temperate needle-leaved forest	45	5 N	123	58 W	10.9	1221	6.2	6.4	-	-
	Hubbard Brook, USA	temperate deciduous forest	43	56 N	71	45 W	5.8	978	6.5	6.2	155.0	112.5
	Pawnee, USA	dry prairie	40	49 N	104	46 W	3.1	401	3.4	-	7.7	-
	San Joaquin, USA	mediterranean grassland	37	6 N	119	44 W	11.2	455	4.1	-	4.9	-
*	Osage, USA (WTG)	warm temperate grassland	36	57 N	96	33 E	14.3	579	4.2	-	5.9	164.4
	Oak Ridge, USA	temperate deciduous forest	35	57 N	84	17 W	13.0	1513	9.4	4.9	92.9	76.1
	Mt. Taylor, USA	douglas-fir forest	35	15 N	107	34 W	8.8	1471	9.6	6.0	153.3	84.8
	Mt. Kasuga, Japan	lucidophyll forest	34	42 N	135	52 E	14.9	1397	6.0	-	175.0	64.0
*	Minamata, Japan (LPF)	lucidophyll forest	32	10 N	130	28 E	17.9	1211	7.7	5.8	197.1	100.5
	Kilbury, India	warm-temperate oak forest	29	24 N	70	28 E	21.9	1427	7.2	-	119.1	-
	Marihan, India	tropical dry forest	25	10 N	82	32 E	25.4	700	6.7	-	28.5	-
	Khao Chong, Thailand	tropical rain forest	7	35 N	100	0 E	26.7	2308	13.0	10.8	178.1	76.0
*	Pasoh, Malaysia (TRF)	tropical rain forest	2	58 N	102	18 E	24.8	1723	10.9	8.0	233.9	79.6
	Manaus, Brazil	tropical rain forest	2	50 S	59	57 W	24.6	3290	10.6	6.0	224.7	150.3
	Nylsvley, South Africa	savanna	24	39 S	28	42 E	17.0	568	4.4	-	15.0	80.0

* detailed-comparison sites

Table 3-3. Site-specific parameter values used in Sim-CYCLE validation run at the four example sites.

Term	Site				
	TRF	LPF	BLF	WTG	
plant parameters				C_3	C_4
ALP	0.10	0.15	0.10	0.25	0.25
CV	0.85	0.85	0.85	0.85	-
KA_0	0.50	0.44	0.52	0.35	0.35
KM_{AE}	0.20	0.30	0.10	0.20	0.05
KM_{CD}	40	40	30	60	5
PC_{SAT0}	40	14	11	14	24
QE_0	0.05	0.05	0.05	0.05	0.05
QT	2	2	2	2	2
$SARG_F$	0.60	0.45	0.21	0.65	0.55
$SARG_C$	0.24	0.23	0.12	0.20	0.25
$SARG_R$	0.31	0.25	0.12	0.20	0.32
$SARM_F$	1.75	1.60	1.01	2.45	2.60
$SARM_C$ (sap)	0.1750	0.1580	0.0580	1.3000	0.7500
(heart)	0.0145	0.0143	0.0033	-	-
$SARM_R$ (sap)	0.5200	0.5030	0.0500	1.0200	0.9000
(heart)	0.0420	0.0423	0.0082	-	-
SLF_F ($x10^{-3}$)	1.05	1.05	1.50	4.95	6.70
SLF_C ($x10^{-3}$)	0.0670	0.0517	0.0020	0.7100	2.2000
SLF_R ($x10^{-3}$)	0.3600	0.3130	0.0071	1.2200	0.6800
T_{OPT}	30	20	18	20	30
T_{MIN}	5	0	-5	0	6
T_{MAX}	45	42	40	40	50
soil parameters					
KM_{SW}	0.18	0.15	0.15	0.30	
KM_{WA}	0.10	0.08	0.09	0.10	
SHR_L	0.50	0.72	1.87	0.87	
SHR_H	0.23	0.30	1.15	0.07	

Table 3-4. Representative estimations in each of four example sites, mostly at the annual base. Calculations were performed under the control climate and 335 ppmv CO_2 condition.

Item	Unit	Site			
		Pasoh TRF	Minamata LPF	Yakutsk BLF	Osage WTG
equilibration time[a]	years	366	467	2450	540
gorss primary production (*GPP*)	Mg C ha^{-1} yr^{-1}	37.2	25.0	3.1	9.7
net primary production (*NPP*)	Mg C ha^{-1} yr^{-1}	10.8	8.3	2.2	4.0
(Miami-model *NPP*)	Mg C ha^{-1} yr^{-1}	9.3	7.5	1.1	4.4
NPP /GPP	-	0.29	0.33	0.70	0.42
leaf area index (*LAI*)	ha ha^{-1}	7.0-7.1	5.8-6.3	0.2-2.3	0.2-1.7
plant carbon stock (*WP*)	Mg C ha^{-1}	248.1	204.7	84.7	5.7
(root:shoot ratio)	-	0.16	0.20	0.84	4.82
soil carbon stock (*WS*)	Mg C ha^{-1}	73.2	102.5	76.8	163.5
total carbon stock (*WE*)	Mg C ha^{-1}	321.3	307.2	161.5	169.2
biomass turnover (*WP /NPP*)	years	23.0	24.8	39.0	1.4
soil turnover (*WS /NPP*)	years	6.8	12.4	35.4	40.4
radiation use efficiency (*RUE*)	g C MJ^{-1}	0.31	0.23	0.15	0.18
water use efficiency (*WUE*)	g C kg^{-1} H_2O	1.34	1.63	1.71	3.04

a time to reach an equilibrium, when annual *NEP* <0.0001 Mg C ha^{-1} yr^{-1}.

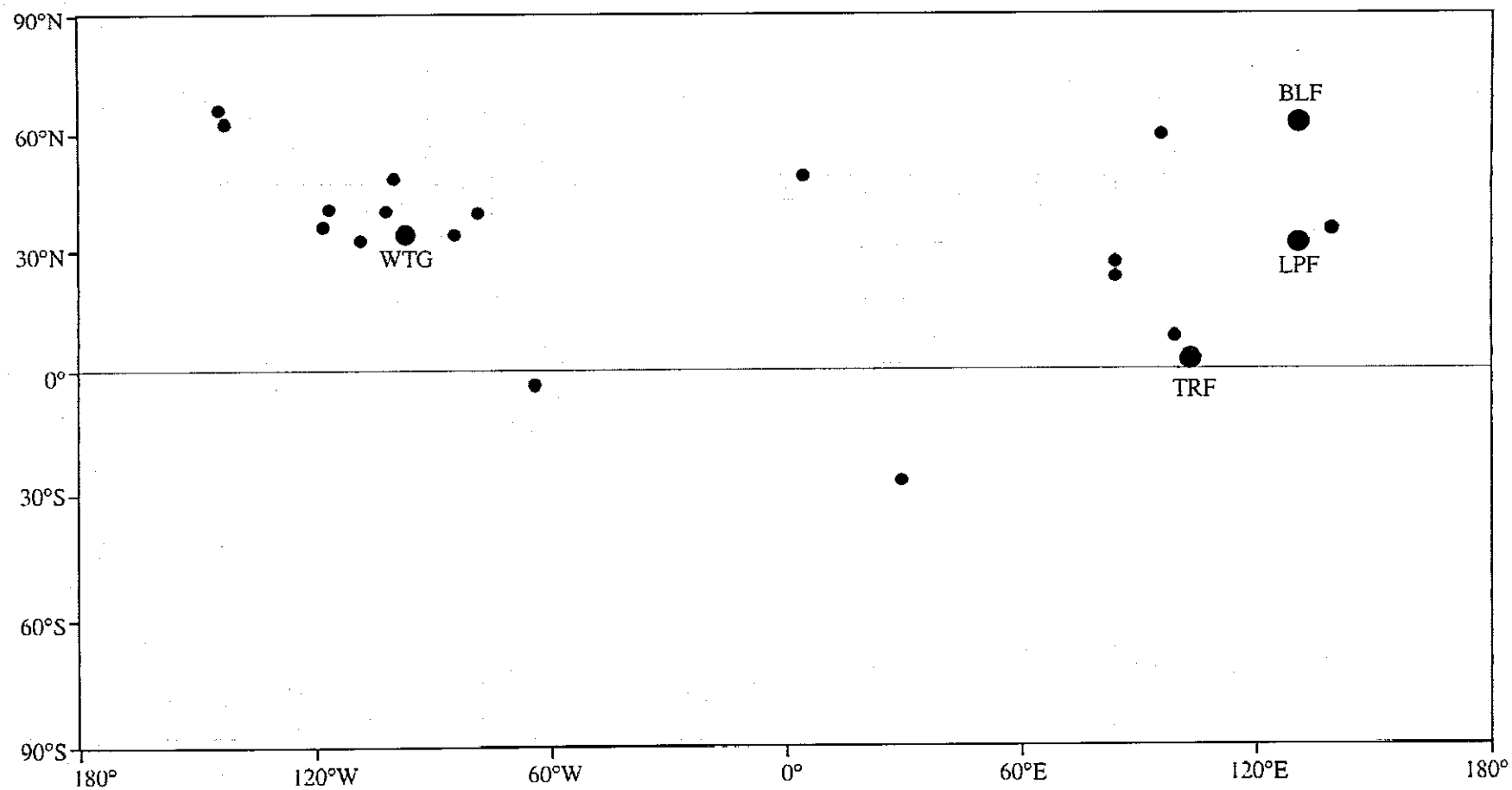

Fig. 3-1. Distribution map of the validation sites. Large circles denote the four selected sites, in which detailed comparison was conducted. Small circles denote the 17 sites, in which approximate comparison was conducted.

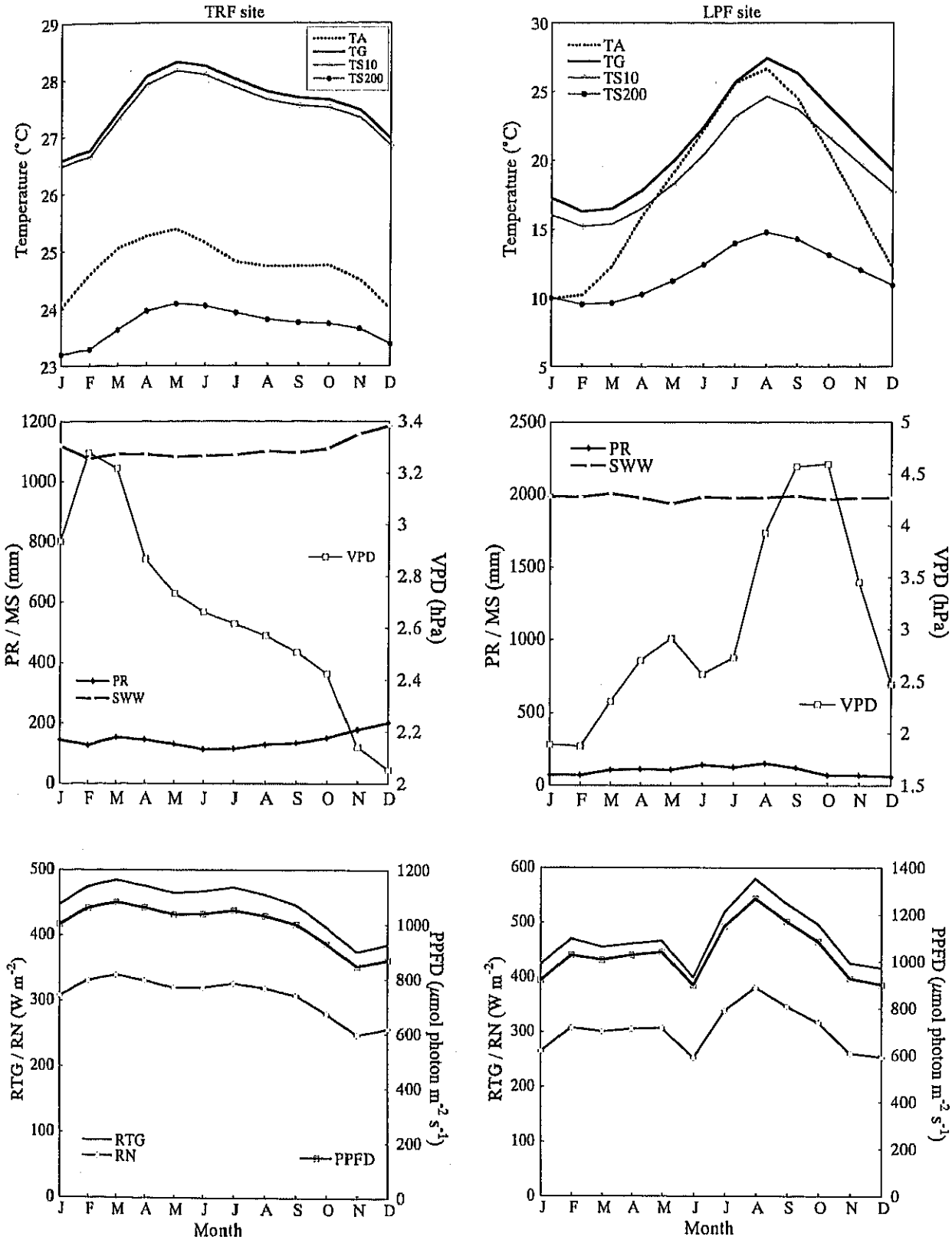

Fig. 3-2. Monthly environmental conditions in the experimental plots. (Upper) Mean air, surface and soil temperatures, (middle) precipitation PR, soil moisture content MS and vapour pressure deficit VPD, and (lower) surface radiation RTG, net radiation RN and photosynthetic photon flux density PPFD. Left, tropical rain forest (TRF); right, lucidophyll forest (LPF).

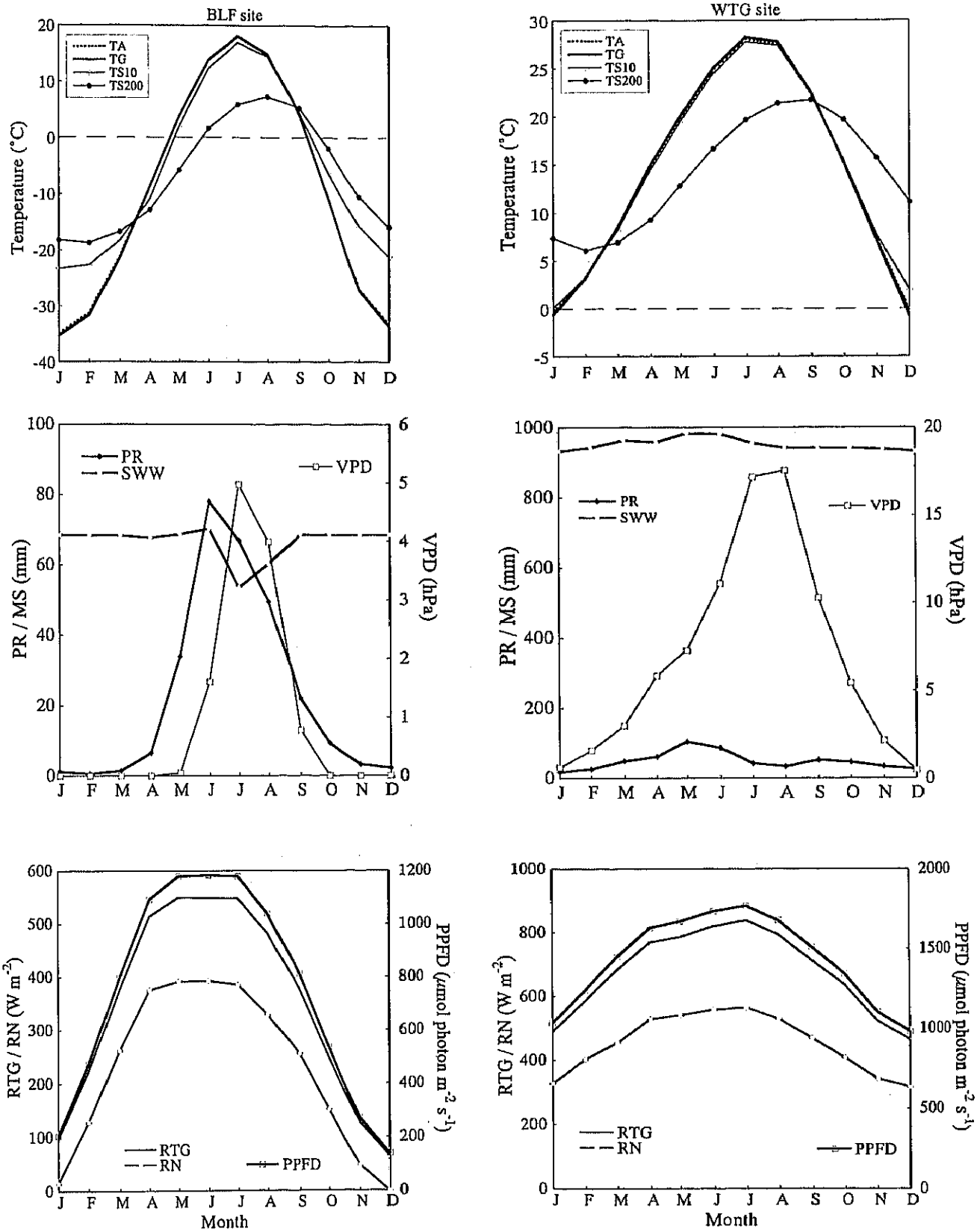

Fig. 3-2 (continued). Left, boreal larch forest (BLF); right, warm temperate grassland (WTG).

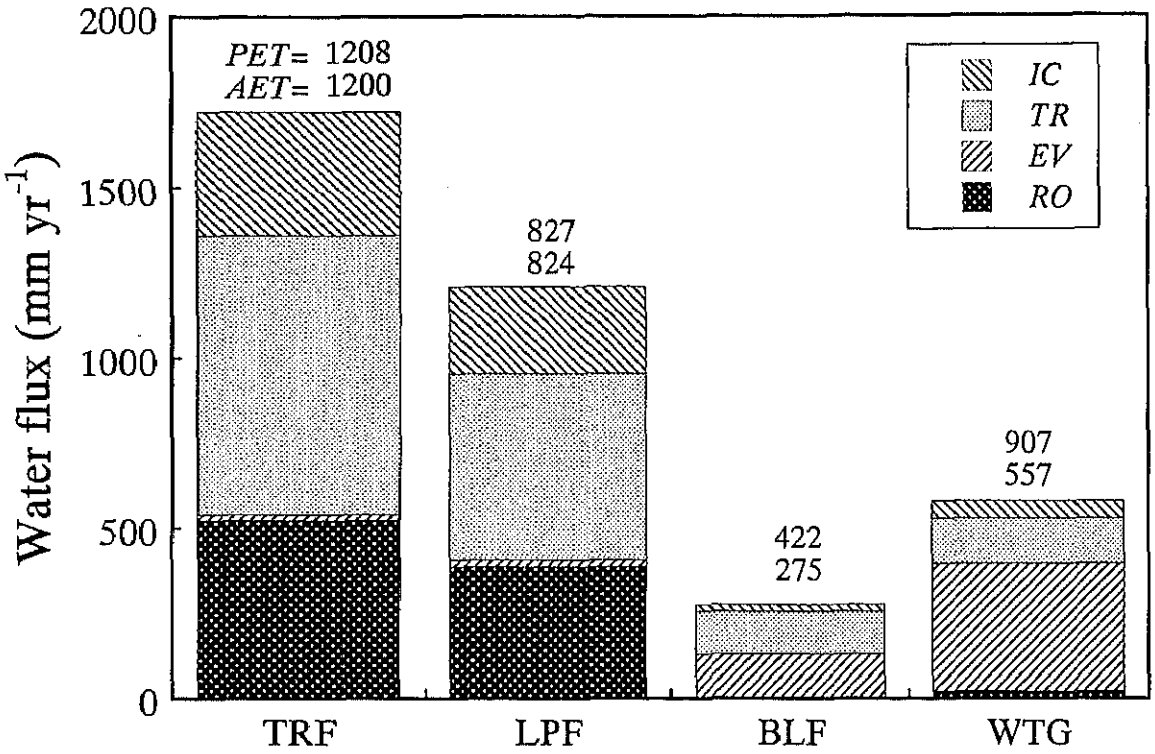

Fig. 3-3. Estimated annual water budget in each of the four example sites. At the equilibrium, change in the soil water content is negligible at the annual base, and precipitation is divided into canopy-interception IC, transpiration TR, evaporation EV, and runoff RO. Annual potential and actual evapotranspiration rates are also shown.

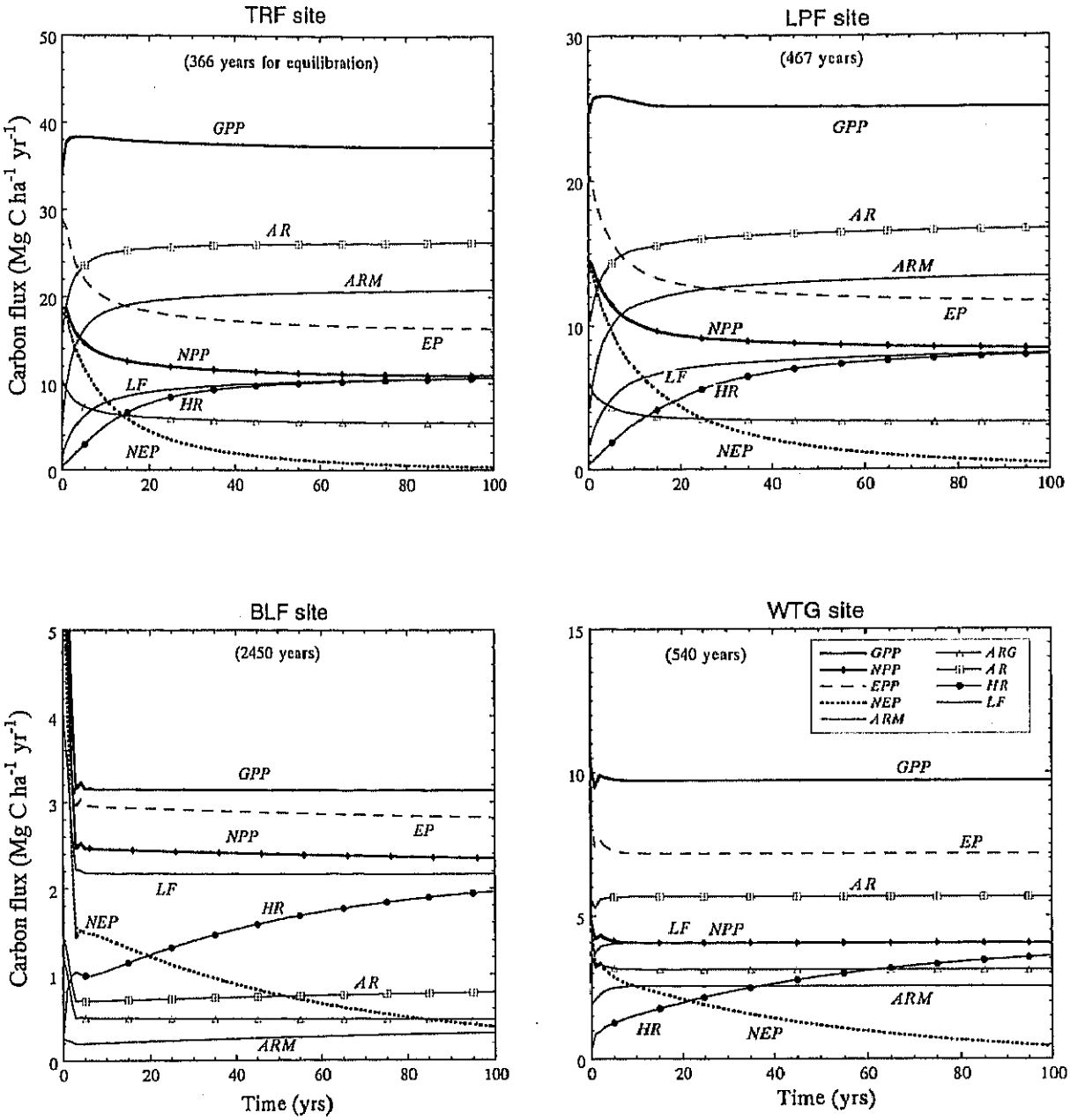

Fig. 3-4. Growth of ecosystem carbon fluxes, estimated by Sim-CYCLE equilibrium run, for the four validation sites. Results for the first 100 years are shown.

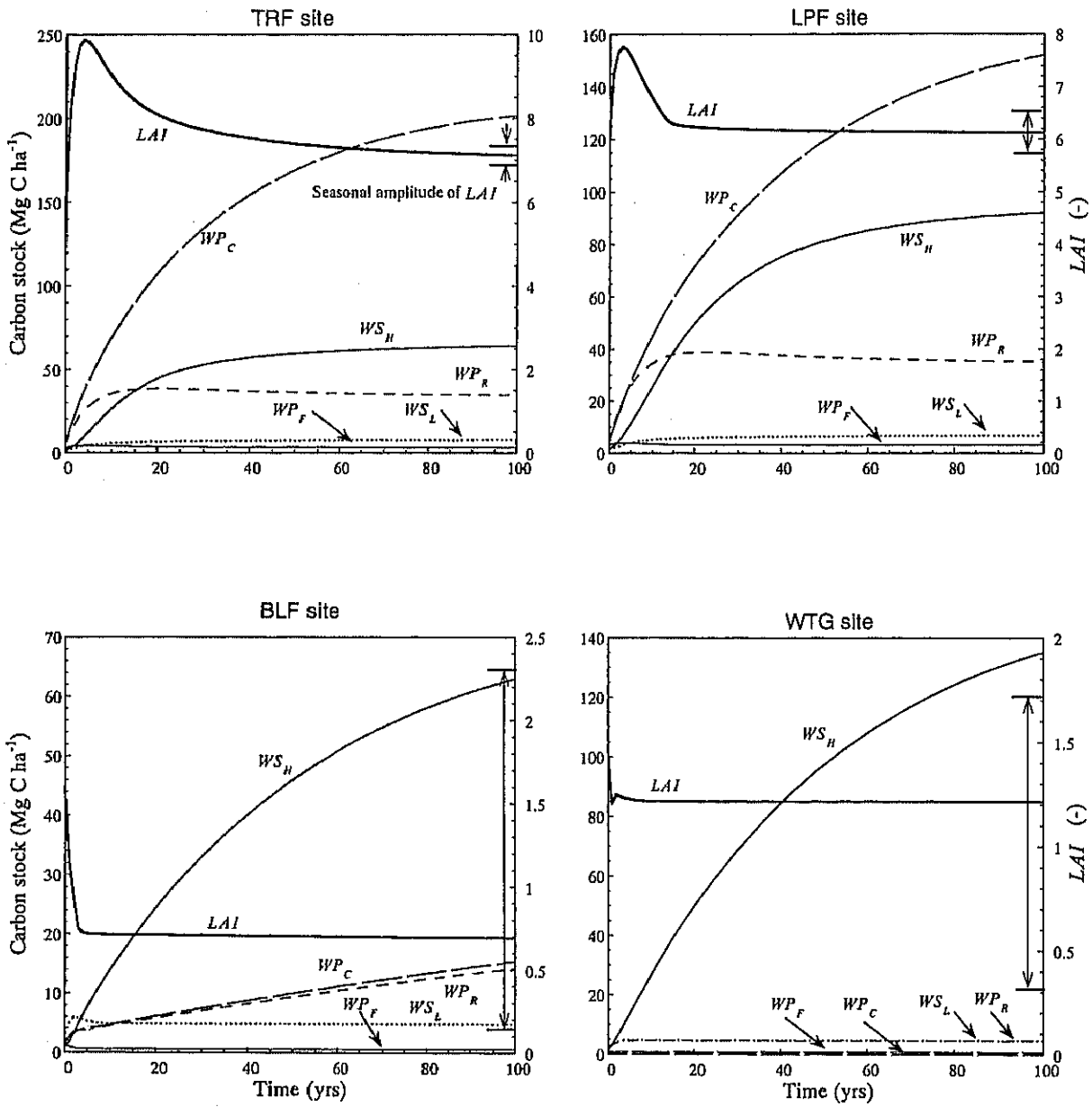

Fig. 3-5. Growth of ecosystem carbon storage, estimated by Sim-CYCLE equilibrium run, for the four validation sites. Results for the first 100 years are shown.

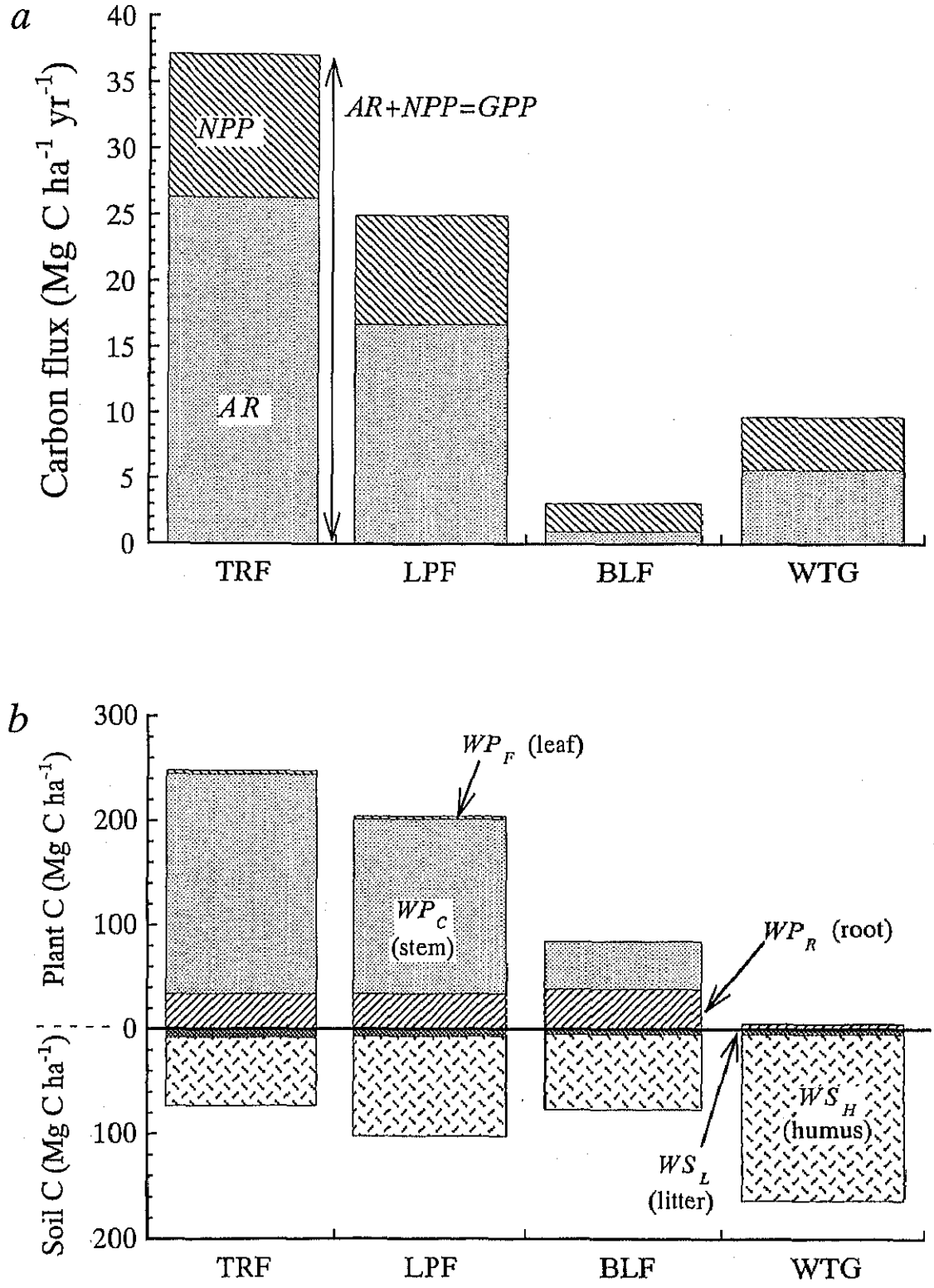

Fig. 3-6. (a) Carbon economy in the four example sites, i.e. fractionation of assimilated carbon GPP into respiration AR and dry-matter prodcuction NPP. (b) Compartment distribution of plant and soil carbon storage in each site, estimated by Sim-CYCLE equilibrium run.

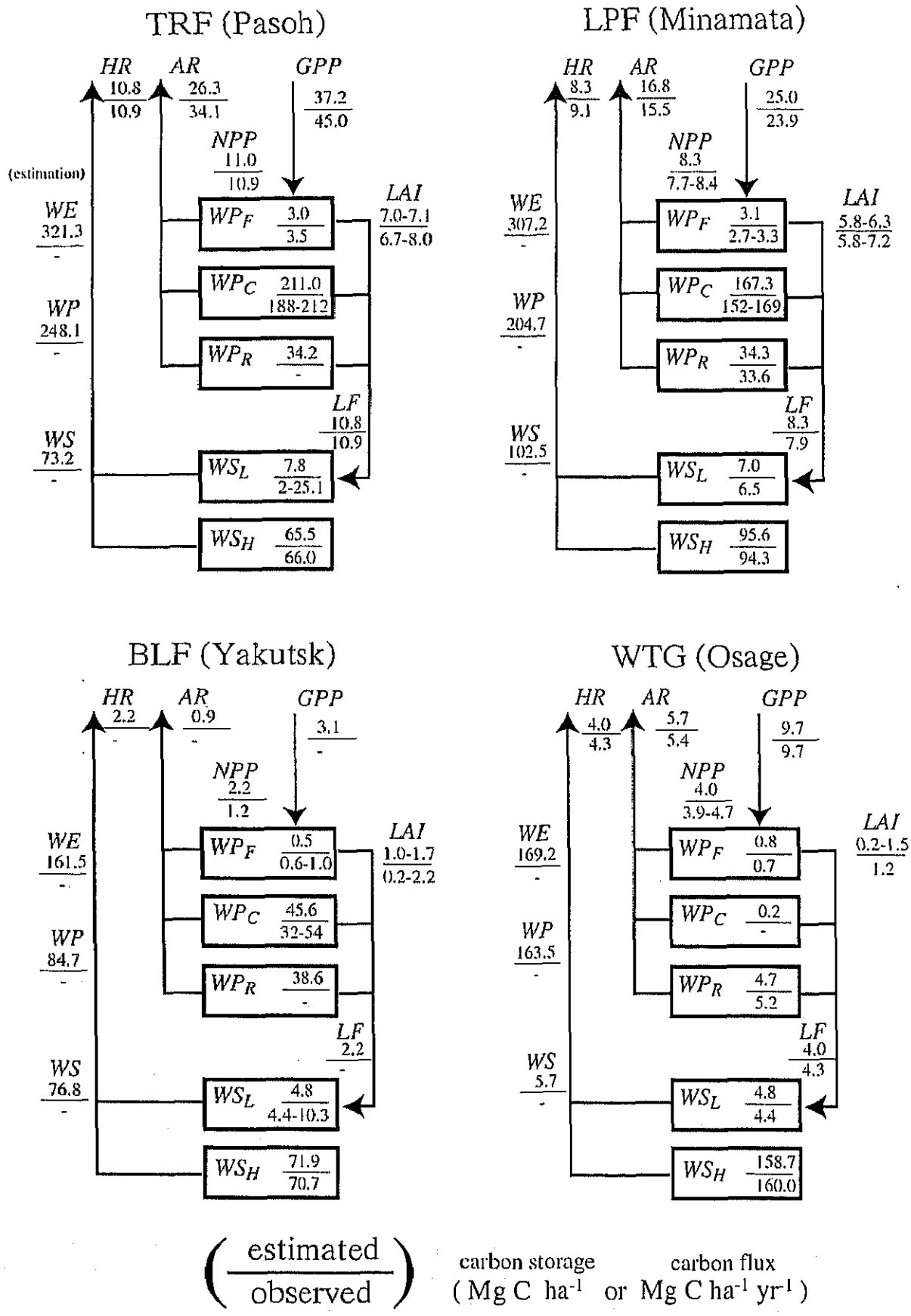

Fig. 3-7. Schematic diagram of carbon dynamics in the four experimental sites. Upper values show those estimated by Sim-CYCLE equilibrium run, and lower values show those observed by field studies (see text).

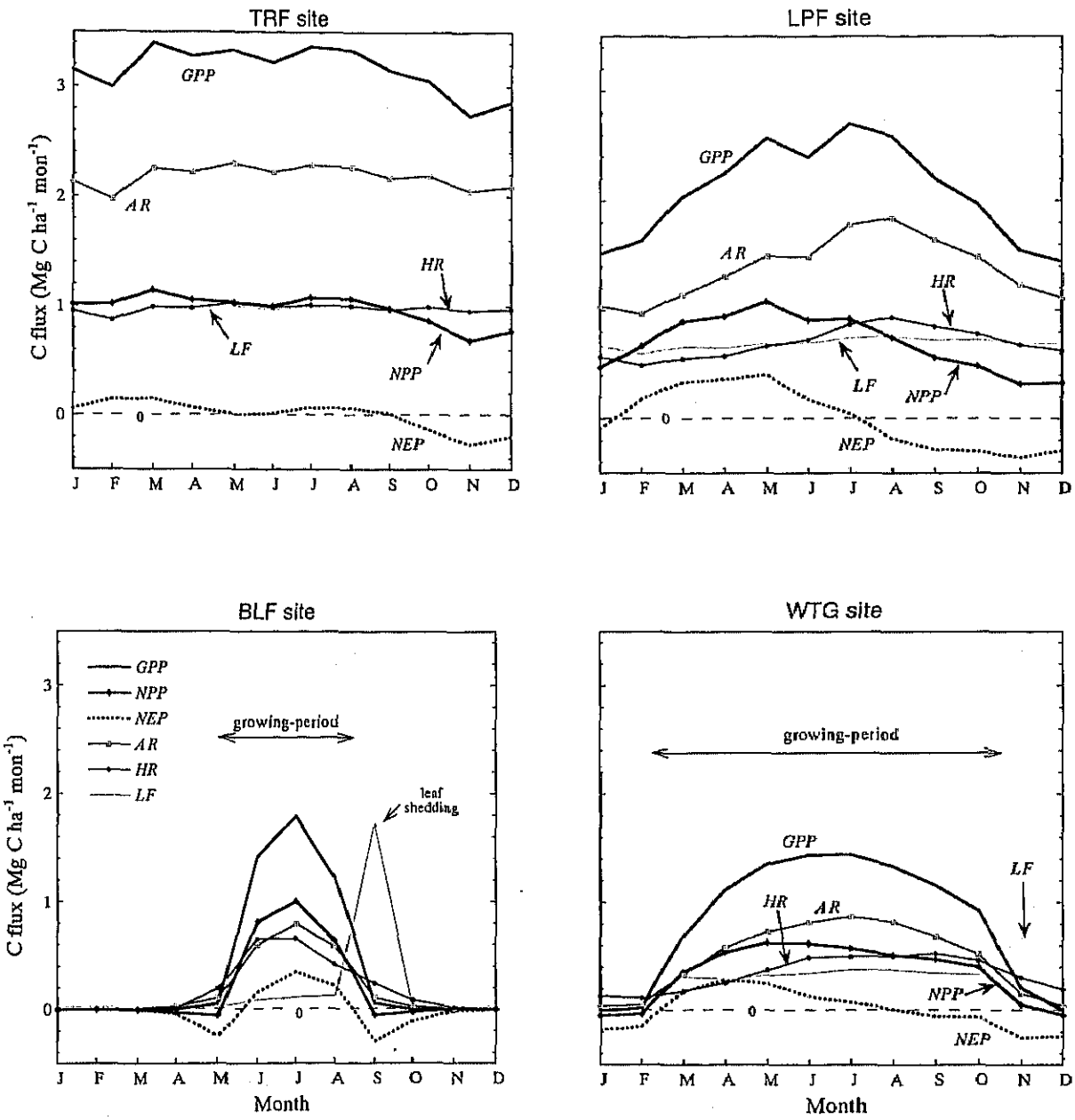

Fig. 3-8. Seasonal pattern of carbon fluxes, estimated by Sim-CYCLE equilibrium run, for the four validation sites.

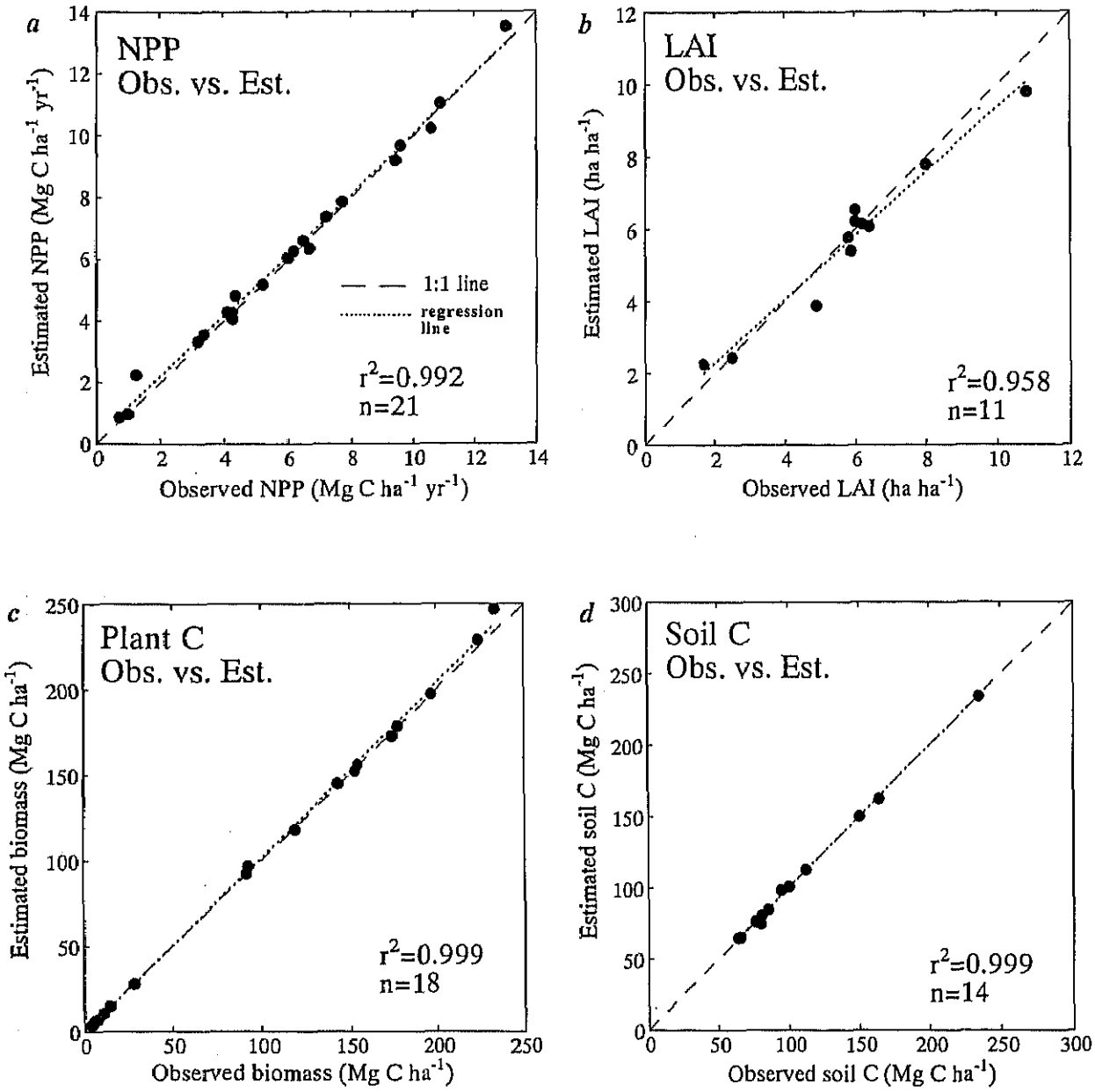

Fig. 3-9. Correlation between model estimation and field observation. (a) Annual NPP, (b) LAI, (c) plant C, and (d) soil C.